Proceedings World Geothermal Congress 2015
Melbourne, Australia, 19-25 April 2015

Fracture Width and Spacing Distributions from Borehole Televiewer Logs and Cores in the Rotokawa Geothermal Field, New Zealand

Cécile Massiot[1], David D. McNamara[2], Andrew Nicol[2] and John Townend[1]

1Victoria University of Wellington, PO Box 600, Wellington 6140, New Zealand; 2GNS Science, PO Box 30-368, Lower Hutt 5010, New Zealand

c.massiot@gns.cri.nz, d.mcnamara@gns.cri.nz, a.nicol@gns.cri.nz, j.townend@vuw.ac.nz

Keywords: statistical fracture analysis, acoustic borehole televiewer logs, cores, Rotokawa Geothermal Field, Taupo Volcanic Zone, New Zealand.

ABSTRACT

The successful targeting of permeable fractures in geothermal fields is aided by understanding the spatial and geometric characteristics of fracture populations. Studies of numerous outcrop, and a limited number of geothermal reservoirs using cores and borehole logs, indicate that fracture frequency and width most commonly follow power-law distributions, with exponential, log-normal, gamma, and power-exponential distributions also reported. This paper presents the first statistical analysis of fracture width and spacing in the high-temperature Rotokawa Geothermal Field, Taupo Volcanic Zone, New Zealand. The fracture dataset comprises: (1) c. 3.6 km of acoustic borehole televiewer (BHTV) logs from three wells and, (2) c. 33 m of core. Statistical distributions have been fitted to the BHTV data using a maximum likelihood estimation method and statistical models selected using the Schwarz Bayesian Criterion. Fracture widths observed on BHTV logs range between c. 1 - 105 mm. Image resolution and sampling bias reduce the useable range of fracture width to less than one order of magnitude (c. 8 - 50 mm). Over this range, considering the sampling effects and core observations, the fracture width is best modelled by an exponential distribution with coefficients between 0.13±0.01 and 0.29±0.02, which should be treated as a lower bound. Analysis of fracture spacing of the four fracture sets identified on BHTV logs indicates that the dominant set (striking NE - SW) is best modelled by a log-normal distribution, while power-law, power-exponential and gamma are also possible for individual wells. These spacing distributions indicate the presence of a characteristic scale which has not been observed in other geothermal reservoirs hosted in crystalline formations. The characteristic scale may be associated with mechanical interfaces associated with stratigraphic layering, faults, or cooling joints and/or sub-horizontal flow-banding in andesitic formations. Stratigraphic layering can consist of a succession of lava flows with intercalated breccia layers in the andesites, welding variations in tuffs and sedimentary layering in the sedimentary formations sampled by the BHTV logs. The subordinate fracture set striking N - S is best modelled by a pareto (power-law) distribution which suggests that the spacing is more likely to be controlled by tectonic processes than by layering. This N - S fracture set is predominant in only one of the wells studied which may indicate a structural control on their occurrence in the vicinity of this well. Low fracture spacing (<0.5 - 5 m) is best modelled by an exponential distribution and higher spacing by log-normal or pareto (power-law) distributions, except for the N – S striking dataset and the NE – SW striking fracture set in well RK32. The change of distribution model at different scales may be linked to the threshold at which fractures start interacting with each other. This work to date underlines the need to combine data spanning a broad range of length scales to conduct a sound statistical analysis of fracture populations and highlights the control on fracture formation by a combination of processes including tectonics, lava cooling and stress perturbations associated with stratigraphic anisotropy. The resulting distributions provide a basis for simulating and calibrating fracture models of geothermal reservoirs beyond those areas directly sampled with BHTV logs or cores and will integrate variations observed over a range of scales between the study wells.

1. INTRODUCTION

Fluid flow is inferred to be controlled by fractures and faults in a number of geothermal systems but the precise locations of permeable structures are often poorly constrained. Fracture models such as Discrete Fracture Networks (e.g., Chiles, 2005; Bonneau et al., 2011) offer a predictive tool for locating fractures which may help to improve the success of well targeting and field management. These fracture models are based on knowledge of the statistical distributions of fracture's geometrical parameters (orientation, length, spacing and aperture) across a range of scales. Hydraulic aperture of fractures is dependent upon the fracture width, i.e. the mechanical aperture (Barton et al., 2013). For the purposes of describing fracture distributions and building models these fracture parameters should be assessed as accurately as possible over a range of scales.

Figure 1a presents the probability density functions (PDF), and mathematical forms of five statistical distributions commonly used to describe fracture width and spacing. Figure 1b shows an example of each distribution for 20 fractures spaced along a hypothetical scanline. Exponential and gamma distributions are formed by a Poisson process where events occur randomly in homogeneous environments (Bonnet et al., 2001 and references therein; Huang and Angelier, 1989). The exponential distribution is a particular case of the gamma distribution where the standard deviation is null. Gamma and log-normal distributions have a low probability at low values of the variable (i.e. either fracture width or spacing in this study). Power-law distributions have a high probability at low values of the studied variable. Fracture populations following a power-law spacing distribution are clustered. The power-exponential distribution is a power-law with an exponential tail. All distributions have characteristic scales except for the power-law which is scale invariant.

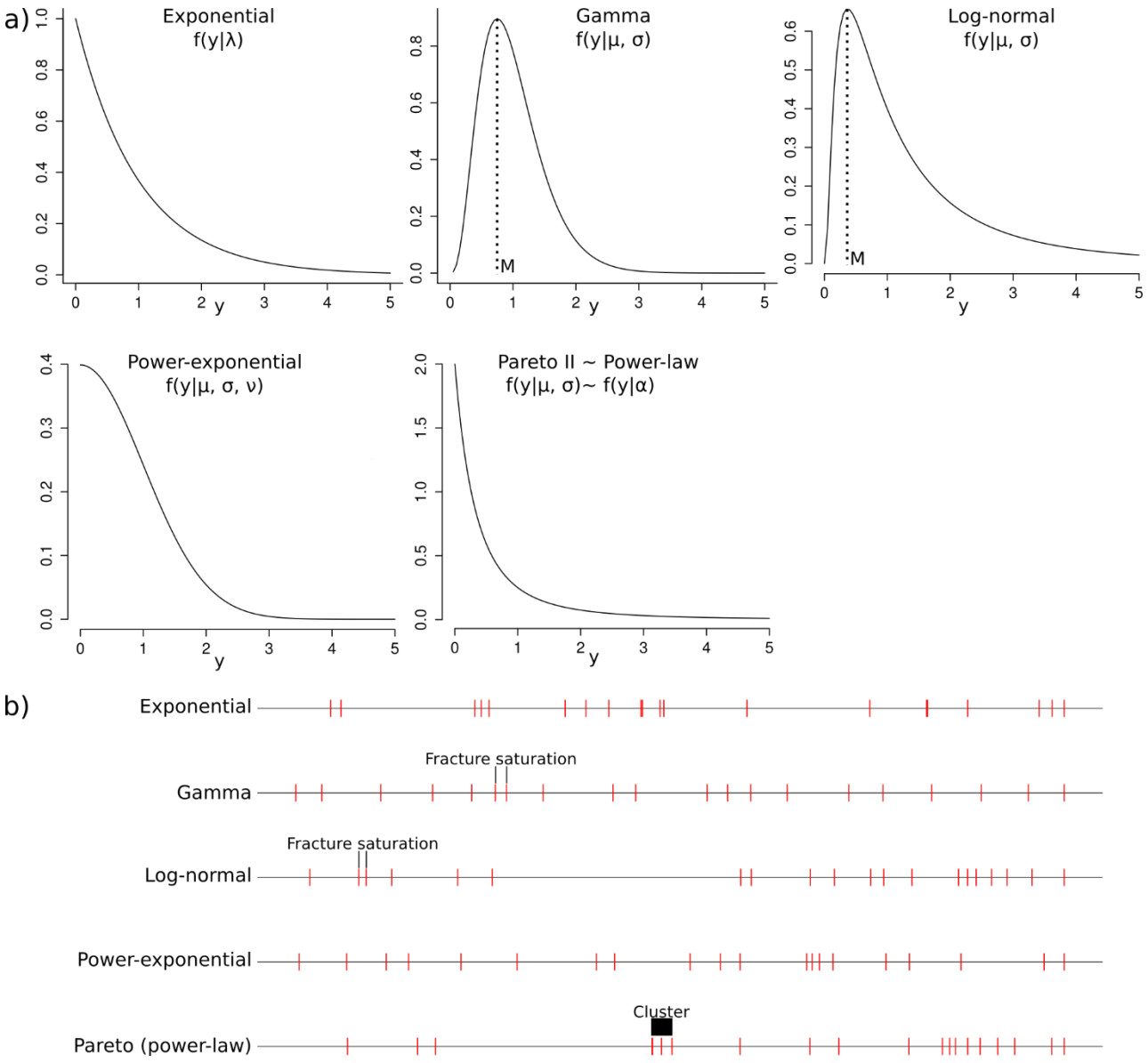

Figure 1 a) Probability density functions for the five distributions evaluated in this study. The mode (M) of the gamma and log-normal distribution for fracture spacing is related to the fracture saturation level. The formulas of each distribution are in Appendix 1. b) Synthetic spacing dataset randomly generated for each distribution. The fracture saturation level is indicated for the gamma and log-normal distribution, and a cluster for the power-law distribution.

Within crystalline-hosted geothermal reservoirs, analysis of acoustic borehole televiewer (BHTV) logs indicate power-law distributions of fracture width and spacing (Barton and Zoback, 1992; Ledesert et al., 1993; Radilla et al., 2012). In other environments, fracture width distributions have been described as log-normal or power-law (Bonnet et al., 2001 and references therein). Spacings of joints (i.e. fractures opening in tension - mode I) have commonly been found to have exponential distributions (Priest and Hudson, 1981; Einstein and Baecher, 1983), log-normal distributions (e.g. Sasaki, 2006, in an epithermal deposit) or regular distributions in well-bedded sedimentary rocks (Ladeira and Price, 1981; Bai and Pollard, 2000). Faults commonly exhibit power-law spacing distributions, even if it may be partially due to sampling bias (Gillespie et al., 1993, Nicol et al., 1996). To date no statistical study of fracture width and spacing have been conducted in an andesite-hosted geothermal reservoir.

The Rotokawa Geothermal Field is located c.14 km north of Taupo, New Zealand, on the eastern side of the Taupo Volcanic Zone (TVZ; Figure 2). Total installed electricity production capacity of 174 MW is produced from two power stations operated by Mighty River Power Ltd.: Rotokawa Geothermal Power Station (34 MW) and Nga Awa Purua power station (140 MW; Legmann and Sullivan, 2003; Horie and Muto, 2010). The stratigraphy comprises volcano-sedimentary and andesitic formations which lack significant fault offset, overlying the faulted Rotokawa Andesite and Mesozoic Greywacke basement (Rae, 2007). The Rotokawa Andesite is an 800 to 2100 m thick unit of andesite lavas and breccias (Rae, 2007). It forms a large buried andesitic volcano with its deeper slopes located under the nearby Ngatamariki Geothermal field (Browne et al., 1992; Chambefort et al., 2014). Within the Rotokawa Geothermal Field, three NE - SW striking normal faults have been inferred based on borehole stratigraphy, reservoir temperatures and microseismicity (Figure 2; Wallis et al., 2013; Sewell, 2013).

The deep, hot (320°C) aquifer at Rotokawa is hosted in the Rotokawa Andesite, which has a low (5 - 10 %) intrinsic porosity (Rae, 2007; Siratovitch et al., 2012; Quinao et al., 2013). Fluid flow in this andesite-hosted reservoir is mostly controlled by fractures and

faults. The reservoir has a heterogeneous permeability distribution, and pressure drawdown analysis reveals that it contains a NE - SW trending barrier to flow related to one of the three main inferred normal faults (Quinao et al., 2012). The heterogeneity of structures and *in-situ* stress orientations is also observed at the borehole scale (McNamara et al., accepted).

The aim of this paper is to characterise the statistical distributions of fracture width and spacing populations observed in cores and BHTV logs from the Rotokawa Geothermal Field. This analysis is intended to serve as the basis for future fracture modelling analyses at the reservoir scale to provide insights into the fluid flow pathways in the reservoir.

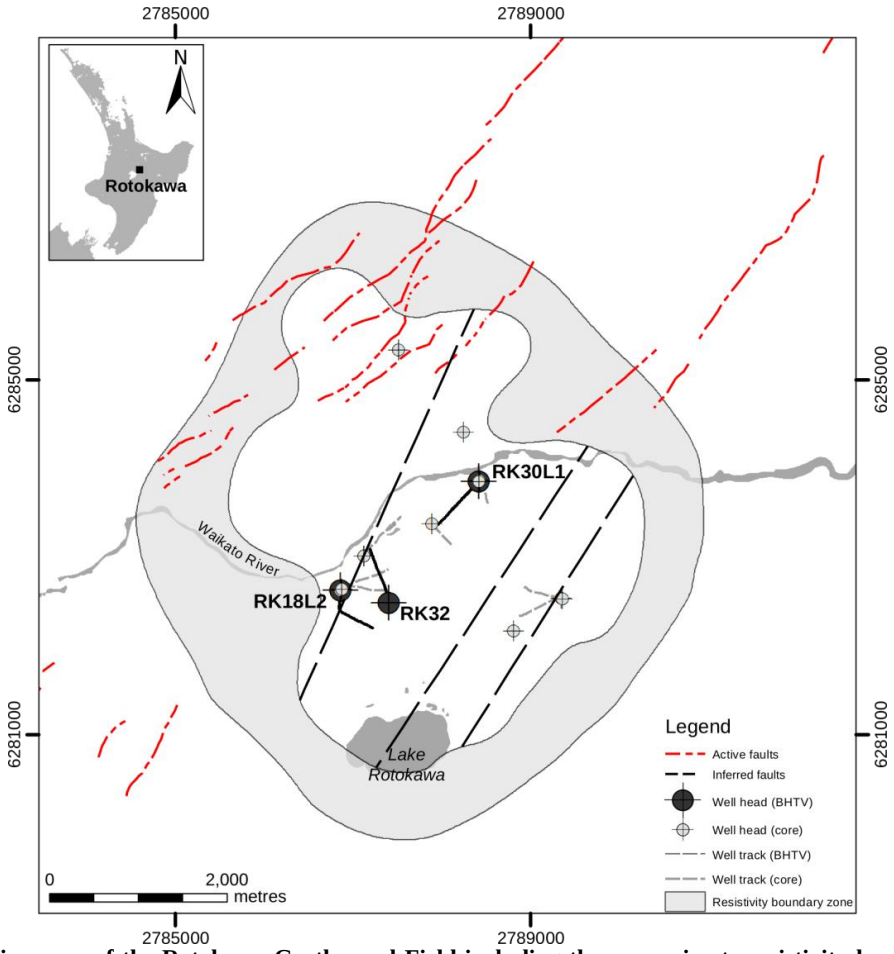

Figure 2: Location map of the Rotokawa Geothermal Field including the approximate resistivity boundary zone at about 500 m depth (after Risk et al., 1992), the mapped active faults (GNS Science active faults database, http://data.gns.cri.nz/af/; Litchfield et al., 2014), the inferred faults projected from the top of the Rotokawa Andesite (Wallis et al., 2013) and the location of the wells where the three BHTV logs and the cores used in this study have been acquired (courtesy of Mighty River Power Ltd.).

2. DATA AND METHODOLOGY

2.1 Acoustic Borehole Televiewer (BHTV) logs

Acoustic borehole televiewer (BHTV) logging yields an image of the inside of a borehole generated by the transmission and reception of ultrasonic pulses. Two types of information are gathered by this technique; the travel time of the sonic wave, which is dependent on the shape and diameter of the well, and the returning amplitude of the wave, which relates to the acoustic impedance of the borehole wall (Davatzes and Hickman, 2010). Planar fractures intersecting a cylindrical borehole appear as sinusoids on BHTV logs, which are automatically oriented to geographic North using inbuilt magnetometers (Figure 3).

Three BHTV logs have been acquired in the Rotokawa Geothermal field (Figure 2) using the high-temperature (300°C) ABI-85 tool, deployed by Tiger Energy Services under the trade name Acoustic Formation Imaging Technology (AFIT). Under typical logging conditions in the TVZ, the BHTV log resolution is c. 5 mm horizontally and c. 10 mm vertically. Resolution is decreased locally by artefacts such as stick-and-pull and poor borehole or logging conditions (Lofts and Bourke, 1999; Massiot et al., 2015). Fractures were identified manually using Recall^{TM} 5.4 software and analysed following the methodology detailed by Massiot et al. (2015). The systematic under-sampling of fractures sub-parallel to the borehole trajectory is mitigated by applying a weighting derived from the angle between the fracture plane and the borehole trajectory (Terzagui, 1965; Massiot et al., 2012). Fracture width is the fracture-normal distance between fracture walls, i.e., measurements have been corrected for fracture dip. In total, 3593 m of BHTV logs were acquired and 1530 fractures identified with high confidence (according to the feature classification in Massiot et al., 2015). A total of 1217 fractures have been located within the 2345 m of the BHTV logs acquired in andesitic formations as defined from cuttings or inferred from nearby wells and 3D modelling (Rae, 2007; Wallis et al, 2013). Other stratigraphic formations sampled by the BHTV logs include the Waikora Formation (greywacke conglomerate) and Tahorakuri Formation (tuff) of the Reporoa Group (Gravley et al., 2006), and the Wairakei ignimbrite (partially welded ignimbrite) which is a member of the Whakamaru group (Rae, 2007).

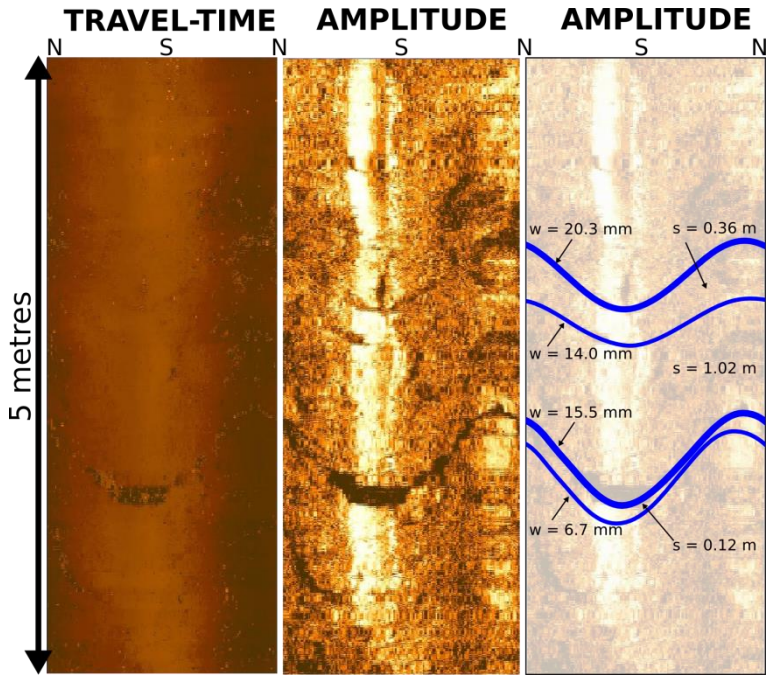

Figure 3: BHTV log with travel-time and amplitude images, and interpretative diagram showing four fractures of varying width (w) and normal spacing (s).

Four fracture sets are identified (Table 1, Figure 4; Allmendinger, 2012). The majority of fractures (FS-1) strike NE – SW, parallel to the maximum horizontal stress (025°±11° to 045°±15°) (S_{Hmax}; confidence intervals are standard deviations; Townend et al., 2012; McNamara et al., accepted), and are steeply dipping (>70°). Fracture set FS-2 is a subordinate grouping striking N – S, observed in wells RK18L2 and RK30L1. Subordinate fracture sets strike NW – SE (FS-3), and NE – SW (FS-4) with more gentle dips (37° – 63°) than FS-1, and are only observed in wells RK30L1 and RK32, respectively.

Fracture width mainly varies between 1 – 57 mm with two wider fractures being 81 and 105 mm, and an arithmetic mean of 10.6 mm. The apparent spacing observed along the well trajectory is converted for each fracture set to the normal spacing orthogonal to the mean fracture set orientation (Priest, 1993). The normal spacing (referred to as "spacing" in the following of the paper) varies between 0 – 58 m with an arithmetic mean of 1.6 m.

Fracture set	**FS-1** (RK18L2, RK30L1 and RK32)	**FS-2** (RK18L2 and RK30L1)	**FS-3** (RK30L1)	**FS-4** (RK32)	**FS-0** (outliers)
Strike orientation	NE - SW	N - S	NW - SE	NE -SW, dipping 45° towards NW	Variable
Number of fractures	923 (791)	141 (128)	71 (58)	73 (70)	464 (308)

Table 1: Orientation and number of fractures identified in the BHTV logs of the Rotokawa Geothermal Field. Well name refers to Figure 2. The number of fractures occurring in the intervals of andesites are indicated in brackets.

2.2 Cores

A total of 33 m of core has been sampled from andesitic formations in 14 wells (Figure 2). The cores exhibit a wide range of alteration intensities (Figure 5a-b) and have two facies: massive lava (Figure 5a-b) and breccia (Figure 5c). The breccias are inferred to either have been inherited from auto-brecciation occurring on the edges of the lava flow during their emplacement, or created by hydrothermal processes. 310 fractures were logged from 21 m of core in massive lava and 35 fractures from 12 m of core in breccia. Fracture width in the cores is between 0.5 – 3 mm, with two fractures being 5 mm wide. The fracture frequency is five times greater in lavas than in breccias in which veins tend to surround clasts (Figure 5c).

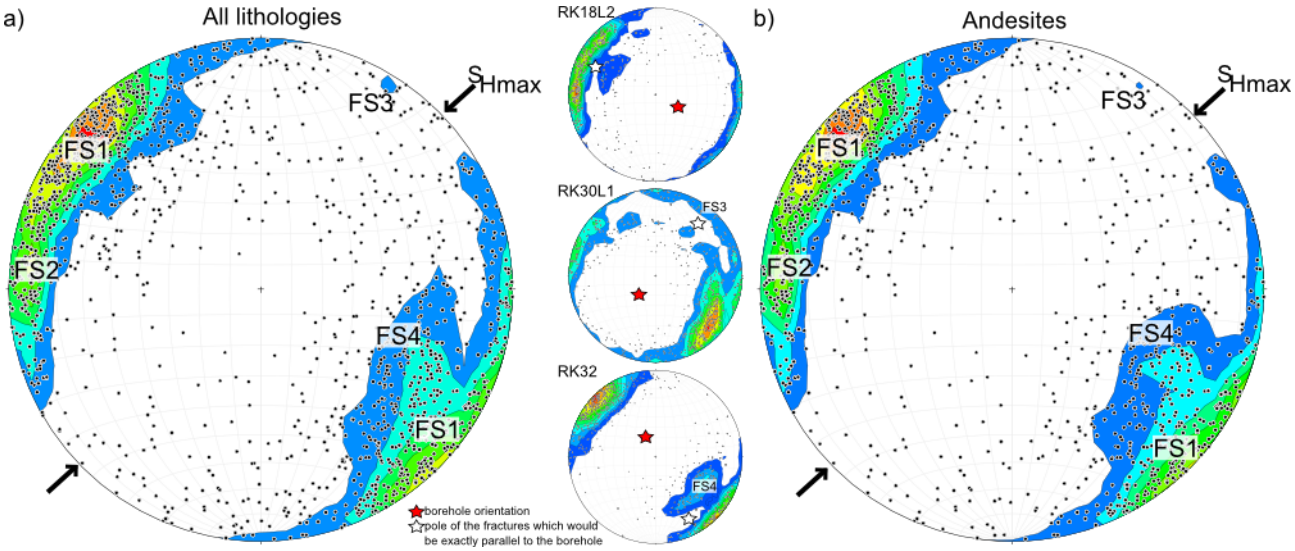

Figure 4: Lower hemisphere stereographic representations of poles to the planes of fractures identified in the three BHTV logs of the Rotokawa Geothermal Field, overlaid by Fisher distribution (1% interval). a) All lithologies, all wells combined, and well by well. b) Andesite intervals. FS-3 and 4 occur only in wells RK30L1 and RK32, respectively, and do not display high Fisher densities on the combined dataset. The S_{Hmax} orientation is derived from McNamara et al. (accepted).

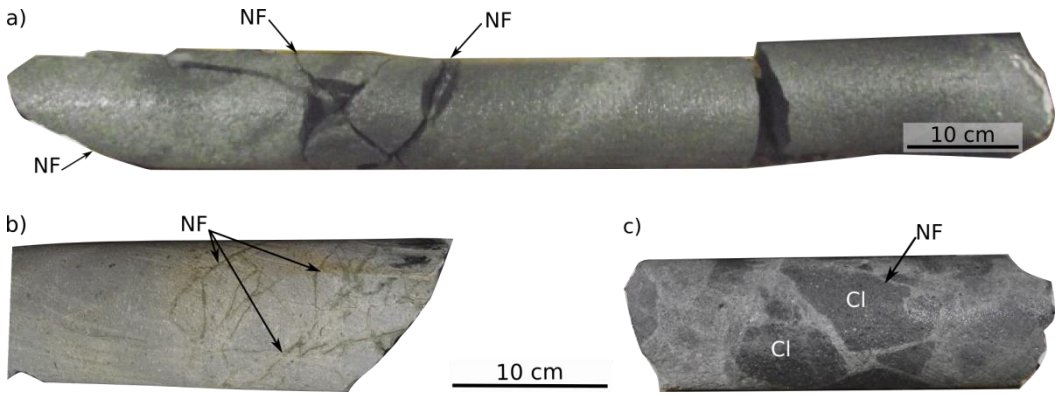

Figure 5: Lithologies observed in cores from the Rotokawa Andesite. a) Moderately altered lava with low fracture density. b) Strongly altered lava, low to high fracture density. c) Moderately altered breccia with low fracture density. (NF: natural fractures, Cl: clast).

2.3 Distribution Fitting Method

Statistical distributions are fitted to the fracture width and spacing data obtained from BHTV log analysis using the Generalized Additive Models for Location Scale and Shape (GAMLSS; Stasinopoulos and Rigby, 2007). This statistical modelling framework uses maximum likelihood estimations and provides more robust estimators than least-squares analysis (Guerriero, 2011; Newman, 2005). GAMLSS is able to evaluate a large series of distribution models which can be highly skewed and/or kurtotic, continuous or discrete. GAMLSS distribution families can be extended by mixing or truncating existing distributions.

The BHTV logs are subject to resolution limits and sampling biases which affect the datasets, in particular towards the low and high values of width or spacing (Pickering, 1995; Barton and Zoback, 1992). Truncation bias reduces the detection of thin or closely spaced fractures. Fractures thinner than the BHTV log resolution of ~5 mm cannot be detected, except in rare cases in which there is a large impedance contrast between the fracture and the borehole wall. Histograms of fracture width (Figure 6a) indicate a paucity of fractures <8 mm wide in wells RK18L2, RK30L1 and the three wells combined, and <9 mm in well RK32. These values are used as truncation thresholds in the respective datasets and thinner fractures are not included in the analysis as they are not fully sampled. Censoring bias relates to the lower probability of intersecting either very wide fractures or large fracture spacings because they are rare. Zuquim and Rowland (2013) reported that extensional fractures in a paleo-hydrothermal system hosted in volcanic formations in the nearby Coromandel area were mostly up to three cm thick while some fractures were up to a few 10's cm. Similarly, from an analysis of 3000 fractures in continuous cores at the Soultz geothermal reservoir, Genter and Traineau (1996) found that the thickest fracture was 25 cm wide but that fractures >10mm wide were rare. Similar observations were made in the BHTV logs where fractures wider than 50 mm are rare (Figure 6a). In addition, apparently wide fractures (>50 mm width) may be composed of several closely-spaced fractures and thus are not included in the fracture width analysis. In summary, the statistical analysis of fracture width was performed over a range of 8 – 50 mm except for well RK32 (9 – 50 mm). These resolution limits are similar to those reported by Barton and Zoback (1992). The truncation limit for the spacing analysis is 0.01 m based on the resolution limit of the BHTV logs and the high probability for more closely spaced fractures to appear as a single fracture. Fractures spaced more than 50 m are rare and censored. The fracture spacing analysis is thus conducted between

0.01 – 50 m. In addition, the changes of fracture spacing at different scales are evaluated by analysing continuous subsets of the measurements covering two orders of magnitude each and separated by half an order of magnitude (i.e. 0.005 - 0.5 m; 0.01 – 1 m; 0.05 – 5 m; etc). The 0.05 – 0.5 m interval may be subject to truncation and is treated with caution.

Five distribution types are evaluated in the fracture width and spacing analysis (Figure 1): exponential, gamma, log-normal, power-exponential and power-law, the latter evaluated in GAMLSS using a pareto Type II distribution. The pareto distribution does not appear as a straight line on a log-log plot but its form and coefficients are directly related to a power-law. To account for data truncation and censoring, the truncated versions of these GAMLSS distribution families were used. The estimated distributions are conditional over the truncated ranges.

The model selection is based on the relative penalized likelihood of the distributions (deviance) using the Schwartz Bayesian Criterion (SBC; Schwartz, 1978). The SBC favours distributions with a higher degree of freedom, i.e. distributions with less parameters (Kolyukhin and Torabi, 2012). The most likely distributions (high SBC rank) have the lowest SBC deviance. The difference between the lowest deviance SBS_{min} and the deviance of the studied distribution SBS_i is evaluated for each dataset:

$$\Delta(SBS_i) = SBS_{min} - SBS_i$$

Fitted distributions with $\Delta(SBS_i)<2$ are likely, while if $\Delta(SBS_i) >6$ they are significantly less likely than the others. All the calculations are performed in the "R" software (R development Core Team, 2008) using the freely available "gamlss" package (Stasinopoulos and Rigby, 2007). The distribution of fracture width and spacing are studied in each of the three wells individually and jointly, and also using data split into fracture sets and/or only within intervals of andesite.

3. RESULTS

3.1 Fracture Width Distribution

Over the range of fracture width considered, for the three wells combined and wells RK18L2 and RK30L1, the exponential and log-normal distributions are found to be the most likely (Figure 6). In well RK32, the log-normal and gamma distributions are the most likely and the exponential is possible in all lithologies albeit less likely (Δ(SBS) = 3.5). The pareto (power-law) distribution is the least likely for all datasets. The exponential coefficient λ (Figure 1; Figure 6; Appendix 1) varies between 0.13 ± 0.01 (in well RK32) and 0.29 ± 0.02 (in well RK18L2; confidence intervals are one standard deviation). The fitting parameters do not vary substantially when considering either all lithologies or the andesites alone (Figure 6).

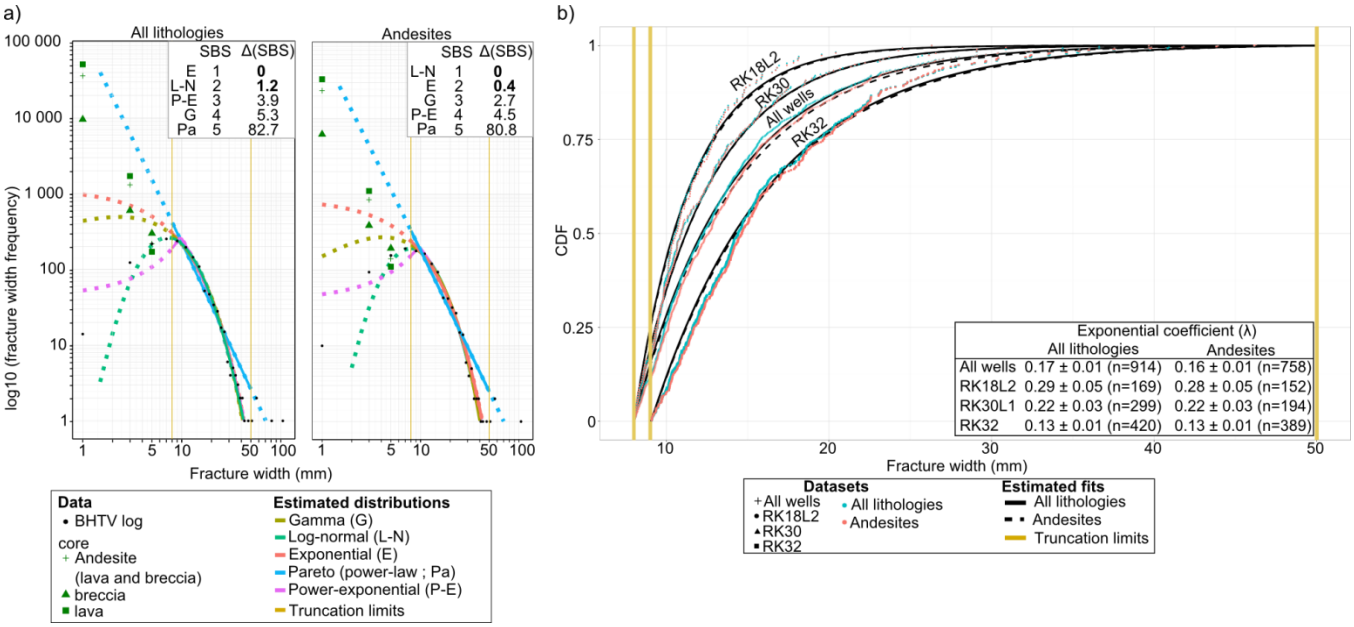

Figure 6: Fracture width and estimated distribution functions. a) Histogram and probability density functions (PDFs), for all lithologies and andesites only in the three BHTV logs (plain line in the width interval used for the distribution fitting). The fracture density in cores, scaled to the overall length of BHTV log, is also displayed. The SBS ranks (1 being the most likely distribution) and difference of SBC deviance (ΔSBC) to the lowest deviance are indicated for each dataset. b) Cumulative Density Function (CDF) of fracture width and estimated exponential distributions, with a list of the coefficient values and their confidence interval (one standard deviation; see appendix 1 for the full mathematical form of the exponential distribution), and the number of fractures (n).

3.2 Fracture Spacing Distribution

Over the 0.01 – 50 m spacing, all fracture sets combined, fracture sets FS-0 (outliers) and FS-1 (NE - SW) are best modelled by a log-normal distribution, for all lithologies or the andesites only (Figure 7). The pareto (power-law) distribution is also likely for these datasets when considering each well separately, as well as power-exponential and gamma for well RK18L2 in fracture set FS-0. Fracture set FS-2 (striking N - S) is best modelled by a pareto (power-law) distribution in both wells RK18L2 and RK30L1, while their combination follows either a pareto (in all lithologies) or a power-exponential distribution (in the andesites only). The N-S fracture set is peculiar as 30% of the fractures are spaced between 0.1 and 0.5 m and the distribution lacks closely spaced fractures (only 9 fractures < 0.1 m). Fracture set FS-3 (NW - SE) is best modelled by a gamma distribution, with log-normal and

pareto also likely for the andesite intervals only. FS-4 (striking NE - SW and gently dipping) is best modelled by either a pareto (power-law) or log-normal distribution.

A change of distribution model occurs between spacings of 0.5 and 5 m (Figure 8). In most datasets, the exponential distribution is the most likely for spacings <1 m (i.e. when considering the spacing ranging 0.005 - 0.5 m and 0.01 – 1 m) while log-normal and in a lesser degree pareto (power-law) or rarely power-exponential are the most likely for higher spacings. The actual limit differs between datasets, e.g. for fracture set FS-1 where it occurs at 0.01 m for the three well combined, 0.05 m for RK30L1 and RK32 and 0.1 m for RK18L2. The following exceptions are observed:

- The most likely distribution for the outliers (FS-0) in RK18L2 varies between each interval, which may be due to the limited size of the dataset (23≤n≤58). This variation is also observed for fracture set FS-2 in wells RK18L2 (29≤n≤108) and RK30L1 in all lithologies (10≤n≤55), for fracture sets FS-3 (10≤n≤54) and FS-4 (15≤n≤53).

- The power-exponential distribution is the most likely at low spacings for fracture set FS-1 in well RK32 (125≤n≤209 between 0.005 - 1 m), FS-2 in the andesites in RK18L2 (55≤n≤91 between 0.005 - 5 m) and RK30L1 (17≤n≤22 between 0.005 - 10 m).

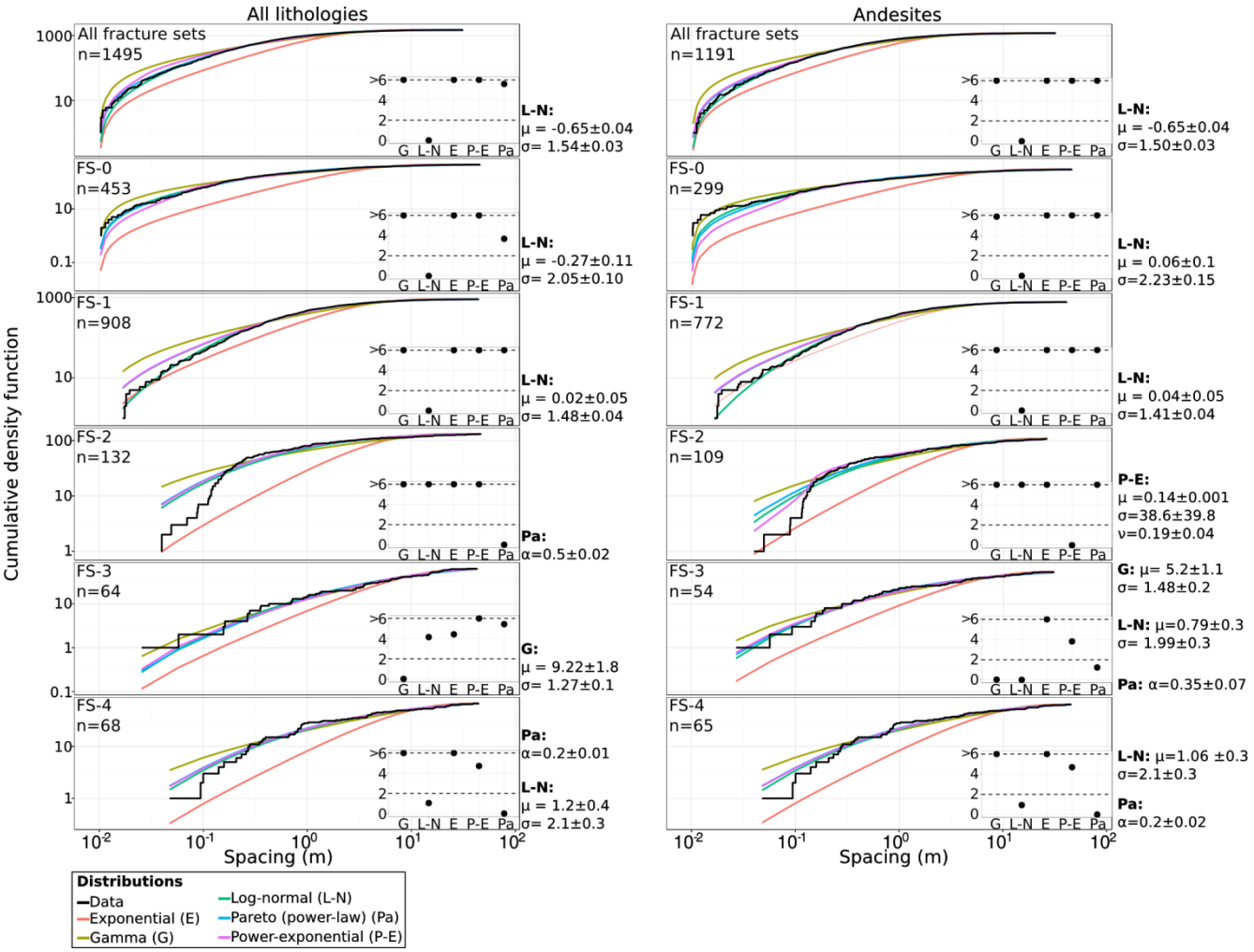

Figure 7: Cumulative fracture density of fracture spacing from the BHTV logs with the estimated fits for the 0.01 - 50 m range, for all lithologies and the andesites only. The difference between the minimum SBC deviance and the deviance of the considered distribution is in insert of each CDF (Δ(SBC) <2 are the most likely). The parameters of each likely distribution is indicated with their confidence interval (one standard deviation). The fracture set numbers refer to Table 1, n is the number of points in the dataset, the full mathematical form of the distribution is in Appendix 1.

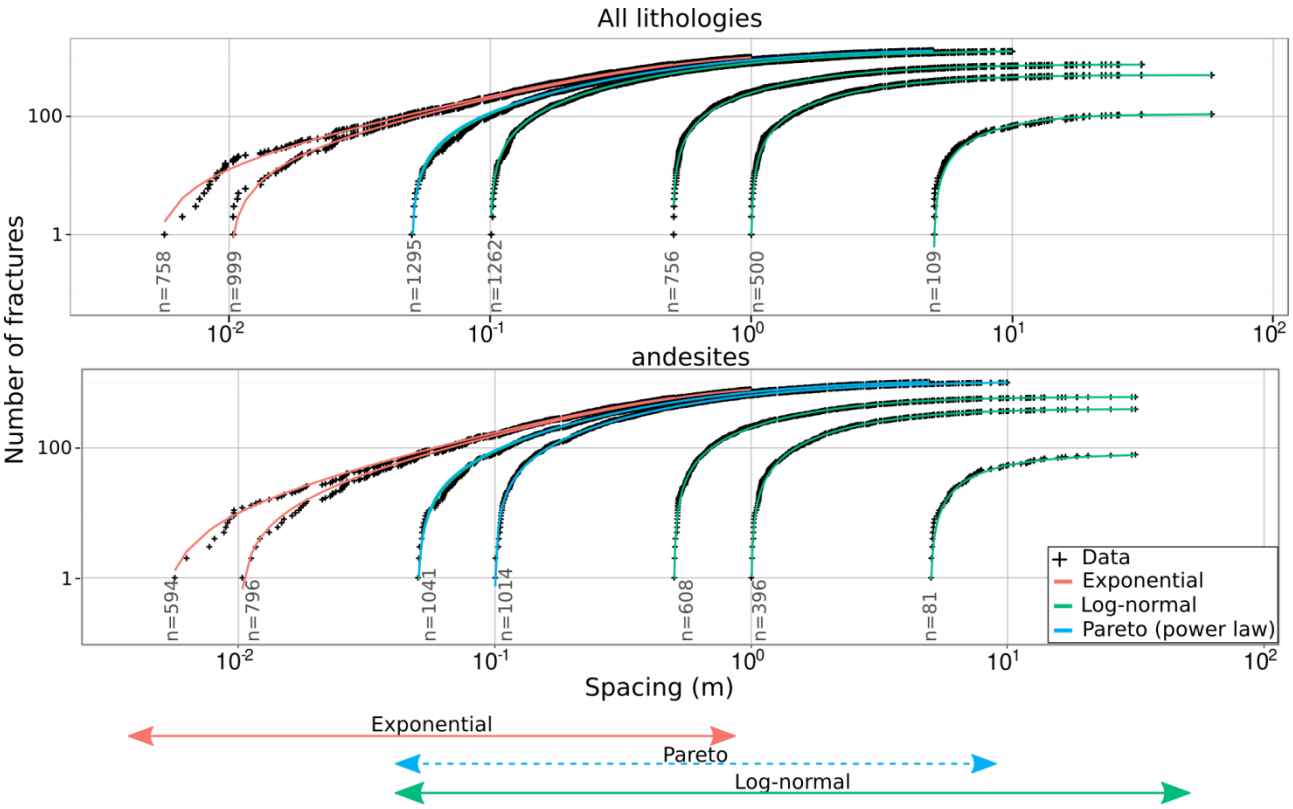

Figure 8: Cumulative fracture density of fracture spacing from the BHTV logs by intervals of two decades for all lithologies and the andesites only, all fracture sets combined, with the cumulative distribution function of the most likely distributions (ΔSBC <2).

4. DISCUSSION

4.1 Fracture Width

Fracture width in BHTV logs is best fitted by log-normal or exponential distributions with similar likelihood for all the datasets considered except well RK32 where log-normal and gamma are the most likely. Log-normal and gamma distribution probability density functions decrease at low values of the variable considered (Figure 1). The analysis of cores indicates that the number of fractures 2 - 4 mm wide, scaled to the length of the BHTV logs, is higher than fractures of 8 - 10 mm wide in BHTV logs by an order of magnitude (Figure 6). The good fits to log-normal and gamma models are thus caused by the observation bias of the BHTV dataset and the exponential model is more realistic for the population as a whole. This behaviour has been observed in previous studies where datasets were restricted to less than one order of magnitude (Pickering 1995).

The probability density function of the exponential distribution fitted to the BHTV data is lower than the number of fractures observed in cores at 1 - 3 mm width (Figure 6). The difference may be due to a change of distribution (e.g., to a power-law) at the different scales, and hence of the fracture mechanisms between 3 - 8 mm. However, it is most likely caused by the different sampling method, as systematic comparison of fracture densities in cores and BHTV logs at the Soultz geothermal field indicates an under-sampling of fractures in BHTV logs by up to 80% (Genter and Traineau, 1992); undersampling was also observed in the TVZ (Massiot et al., 2015).

The exponential coefficient λ is similar in wells RK18L2 (0.29±0.05) and RK30L1 (0.22±0.03), higher than in the combined dataset (0.17±0.01) and well RK32 (0.13±0.01). The coefficients are very similar when considering all lithologies or only the andesite intervals, which is likely due to the fact that 83% of the fractures are located within the andesites. The variation of λ coefficient may reflect structural changes across the field with a higher proportion of thin fractures in wells RK18L2 and RK30L1 than in well RK32. The lower λ coefficients also coincides with the larger datasets, which may have affected the estimation.

Taking into consideration the various biases described, the fracture width is inferred to follow an exponential distribution. The exponent λ varies between 0.16 and 0.23 and, in view of the order of magnitude difference of frequencies between the cores and the BHTV logs, should be treated as a lower bound.

These results are different from those of other studies in crystalline geothermal where fracture width was found to be power-law (Ledesert et al., 1993; Radilla et al., 2012; Barton et al., 2013). The occurrence of the exponential distribution indicates that there is a characteristic fracture width (Bonnet et al., 2001 and reference therein). If such a characteristic fracture width exists (rather than being due to sampling artefacts and the limited range of observations to less than one order of magnitude), it could be due to a number of factors, such as the thickness of lava flows and interlayered breccias in andesitic formations and their influence on the propagation and thickening of fractures.

4.2 Fracture Spacing

Fracture spacings of 0.01 - 50 m are not significantly affected by sampling bias, and are considered to be reasonably representative of spacing in the reservoir over 3.5 orders of magnitude. The spacing of all fracture sets, apart from FS-2, are best modelled by distributions having a characteristic scale, i.e. log-normal, power-exponential or gamma. The characteristic scale can be linked to thermal, mechanical or lithological processes in the reservoir (Bonnet et al., 2001 and references therein). Log-normal and gamma distributions have been reported in layered formations where fractures are strata-bounded (Huang and Angelier, 1989; Hooker et al., 2013). In these conditions, the low probability of small spacing may be related to stress shadow effect which prevents the initiation of new fractures in the vicinity of existing fractures (Wu and Pollard, 1995; Figure 1b). Outcrop studies of paleo-hydrothermal systems in the nearby Coromandel peninsula hosted in andesitic formations have highlighted the higher degree of control of pre-existing joints over faults for the development of veins (Brathwaite et al., 2001). Recently, Zuquim and Rowland (2013) reported that hydrothermal breccias tend to be strata-bounded in rhyolitic flows where flow-banding is sub-horizontal. In contrast to crystalline rocks where power-law fracture spacing have been reported (Barton et al., 1992; Ledesert et al., 1993), fracture spacing for the Rotokawa Geothermal Field is dominated by characteristic scales which could be due to the influence of mechanical layering and/or pre-existing cooling joints on the fracture network geometry.

In the andesites, the log-normal coefficients of fracture set FS-1 (striking NE - SW) vary from -0.16±0.13 to 0.70±0.13 and 1.28±0.05 to 1.56±0.1 for μ and σ, respectively (see Appendix 1 for the full mathematical form). These scales may represent mechanical interfaces related to the spacing of cooling joints (centimetric to metric; Sporli and Rowland, 2006), bounding by the intrinsic flow-banding, the intercalation of breccia layers between massive lava flows (5 - 30 m thick) or the presence of faults in the vicinity of the wells not resolved in the field scale structural model (McNamara et al., accepted). In the other formations, the characteristic scale could be related to the successive tuff layers in the Wairakei Ignimbrite and Tahorakuri Formation with various degrees of welding, hence mechanical properties, or to sedimentary layers in the Waikora Formation.

Fracture set FS-3 (striking NW - SE, parallel to S_{hmin}) is best modelled by a gamma distribution, although log-normal and pareto (power-law) distributions are also likely for the andesite intervals only. As only 64 fractures were occurring in the fracture set FS-3, this fit is less reliable than the estimates of fracture models for other sets, although gamma distributions of joint spacing have been reported in layered formations (Huang and Angelier, 1989). Fracture set FS-3 may consist of joints where the characteristic length (μ between 5.2±1.1 - 9.2±1.8 and σ between 1.3±0.1 - 1.5±0.2) is controlled by the thickness of the layers. The gamma distribution is the most likely when considering all lithologies, including the layered volcano-sedimentary Waikora Formation, Tahorakuri Formation and Wairakei Ignimbrite where the stratigraphic layering may exert a higher control on the fracture spacing.

Fracture set FS-2 (N - S) has a distinct orientation from FS-1 (NE - SW) in well RK18L2 (Figure 4a). The distinction between FS-1 and FS-2 fracture sets is less clear in well RK30L1. Fracture set FS-2 is best modelled by a pareto (power-law) distribution in well RK18L2, while power-exponential, log-normal and gamma distribution families are also possible in well RK30L1. This difference between wells may be due to the proximity of well RK18L2 to an inferred fault oriented at 024°/89° SW (Figure 2; Wallis et al., 2013) which may locally promote the generation of a power-law distribution fracture spacing population. *In-situ* stress orientation rotations occur in this well and have been linked to the effect of active faulting in the vicinity (McNamara et al., accepted).

Power-law distributions are devoid of characteristic scale and indicate clustering (Figure 1b). Fracture set FS-2 in well RK18L2 is best modelled by a power-law and thus may not be as affected by intrinsic layering of the andesites as other fracture sets. The N - S striking orientation of fracture set FS-2 at c. 30° from S_{Hmax} may also indicate that this fracture set is more favourably oriented for shear failure and critically stressed (Barton et al., 1995). The α power-law exponents of fracture set FS-2 vary between 0.5±0.02 and 0.65±1.58 in wells RK18L2 and RK30L1, respectively, a significantly smaller range than the other fracture sets where the pareto distribution is likely (0.17±0.01 to 2.2±4.3), and are similar to those reported by Radilla et al. (2012). Power-law distributions of fracture attributes are often associated with the power-law cumulative density function for earthquake magnitudes which reflect the scale invariance of the fault rupture sizes and has a slope called "b-value" in log-log plots. The power-law exponents of the fracture spacing of FS-2 are similar to b-values of 1.0 - 1.1 found in earthquake studies in the TVZ (Hurst et al., 2008).

The change in fracture distribution model for the small (exponential) and higher (log-normal, power-law or power-exponential) spacing occurring between 0.5 - 5 m (Figure 8) is consistent with observations made on the evolution of fracture systems. Rives (1992) observed that the spacing of joints in layered sedimentary formations and analogue experiments evolves from an exponential to a log-normal distribution as the system matures, until reaching a normal distribution at the fracture saturation level. Similar processes may occur at Rotokawa where closely-spaced fractures (<0.5 to 5 m) nucleate randomly in a locally homogeneous formation and stress field, while the spacing of more widely-spaced fractures is controlled by pre-existing joints, layering and/or tectonic forces. The limited size of the dataset prevents any firm conclusion on individual fracture sets. In any case, it is clear that the fracture network in the Rotokawa Geothermal Field has a scale hierarchy and cannot be treated similarly at different scales.

4.3 Implications for Fluid Flow in the Rotokawa Reservoir

The analysis of the fracture width and spacing conducted to date indicates that the andesite-hosted Rotokawa Geothermal reservoir has characteristic sizes controlling the fracture distributions in the reservoir, contrary to findings from geothermal fields hosted in crystalline formations. Variations of distribution models and coefficients are observed between wells and fracture sets. Despite the high number of fractures observed in the BHTV logs, only a subset occur in permeable zones (McNamara et al., accepted). Numerous fractures controlled by a combination of stratigraphic and tectonic processes may form part of the backbone of the network with temporarily open and interconnected fractures. These characteristics, as well as the change of fracture distribution at various scales, and the variations observed between fracture sets, will be included in fracture and fluid flow models.

CONCLUSION

Three BHTV logs and 23 cores acquired in the Rotokawa Geothermal Field have been analysed to characterise the fracture width and spacing geometrical parameters. Five statistical distributions are fitted with a maximum likelihood algorithm. The combination

of BHTV log and core data indicate that fracture widths between 8 or 9 and 50 mm are best modelled by an exponential distribution. The exponential exponent varies from 0.16 to 0.23 and is considered a lower bound. Relatively higher fracture frequencies of narrow fractures (1 - 3 mm) in cores than in BHTV logs is likely related to the different sampling method. The presence of a characteristic size in the exponential distribution suggests an intrinsic layering of the formations affecting the fracture thickening. The fracture spacing also has characteristic scales and is best represented by a log-normal, power-exponential or gamma distribution, suggesting a control on fractures by mechanical layers such as faults, pre-existing cooling joints, flow-banding and/or lava flow boundaries with intercalated breccia layers. Fracture set FS-2 in well RK18L2, oriented N - S is best modelled by a power-law with a 0.5 - 0.6 coefficient (on cumulative density functions) and may consist of tectonic fractures less affected by the formation layering than the other fracture sets. A change of statistical model for fracture spacings from the exponential at <0.5 - 5 m to log-normal and pareto (power-law) distributions at higher spacings reflect a change of fracture processes at different scales. The presence of layers and/or pre-existing cooling joints, as well as the variation of fracture characteristics across field and between fracture sets have direct impacts on the fracture processes and associated permeability occurring in the Rotokawa Geothermal Reservoir and will be included into reservoir-scale fracture models.

ACKNOWLEDGEMENTS

This project forms part of the first author's PhD thesis funded by the Sarah Beanland Memorial Scholarship awarded by GNS Science. The authors would like to thank the Rotokawa Joint Venture Ltd. (Mighty River Power Ltd. and Tauhara North No.2 Trust) for allowing publication of this work.

REFERENCES

R.W. Allmendinger, N. Cardozo, D.M. Fisher. Structural Geology Algorithms: Vectors and Tensors. *Cambridge University Press* (2012).

Bai, T., Pollard, D.D.: Fracture spacing in layered rocks: a new explanation based on the stress transition. *Journal of Structural Geology*, **22**, (2000), 43–57

Barton, C.A., Zoback, M.D.: Self-similar distribution and properties of macroscopic fractures at depth in crystalline rock in the Cajon Pass scientific drill hole. *Journal of Geophysical Research*, **97**, (1992), 5181–5200.

Barton, C.A., Moos, D., Hartley, L., Baxter, S., Foulquier, L., Holl, H., Hogarth, R., Hogarth, R., Study, C., Field, H.: Geomechanically coupled simulation of flow in fractured reservoirs. *Proceedings*, Thirty-Eighth Workshop on Geothermal Reservoir Engineering, Stanford University, Stanford. (2013).

Barton, C.A., Zoback, M.D., Moos, D.: Fluid flow along potentially active faults in crystalline rock. *Geology*, **23**, (1995), 683.

Bonnet, E., Bour, O., Odling, N.E., Davy, P., Main, I., Cowie, P., Berkowitz, B.: Scaling of fracture systems in geological media. Reviews of Geophysics, **39**, (2001), 347–383.

Bonneau, F., Henrion, V., Caumon, G., Renard, P., Sausse, J.: A methodology for pseudo-genetic stochastic modeling of discrete fracture networks. *Computer and Geosciences* **56**, (2013), 12–22.

Brathwaite, R.L., Cargill, H.J., Christie, A.B., Swain, A.: Lithological and spatial controls on the distribution of quartz veins in andesite- and rhyolite-hosted epithermal Au-Ag deposits of the Hauraki Goldfield , New Zealand. *Mineralium Deposita*, **36**, (2001), 1–12.

Browne, P.R.L., Graham, I.J., Parker, R.J., Wood, C.P.: Subsurface andesite lavas and plutonic rocks in the Rotokawa and Ngatamariki geothermal systems, Taupo Volcanic Zone, New Zealand. *Journal of Volcanology and Geothermal Research*, **51**, (1992), 199–215.

Chambefort, I., Lewis, B., Wilson, C.J.N., Rae, A.J., Coutts, C., Bignall, G., Ireland, T.R.: Stratigraphy and structure of the Ngatamariki geothermal system from new zircon U-Pb geochronology: Implications for Taupo Volcanic Zone evolution. *Journal of Volcanology and Geothermal Research*, (2014), in press.

Chiles, J.: Stochastic modeling of natural fractured media: a review. In: Leuangthong, O., Deutsch, C.V. (Eds.), Geostatistics Banff 2004 of Quantitative Geology and Geostatistics, **14**. Springer, (2005), pp. 285–294

Davatzes, N.C., Hickman, S.: Stress, fracture, and fluid-flow analysis using acoustic and electrical image logs in hot fractured granites of the Coso Geothermal Field, California, U.S.A., *in: Poppelreiter, M., Garcia-Carballido, C., Kraaijveld, M. (Eds.), Dipmeter and Borehole Image Log Technology: AAPG Memoir 92.* (2010) pp. 259–293.

Einstein, H.H., Baecher, G.B.: Probabilistic and Statistical Methods in Engineering Geology. *Rock Mechanics and Rock Engineering*, **16**, (1983), 39–72.

Genter, A., Traineau, H.: Analysis of macroscopic fractures in granite in the HDR geothermal well EPS-1 , Soultz-sous-Forets , France. *Journal of Volcanology and Geothermal Research*, **72**, (1996), 121–141.

Gillespie, P.A., Howard, C.B., Walsh, J.J., Watt, J.: Measurement and characterisation of spatial distributions of fractures. *Tectonophysics*, **226**, (1993), 113–141.

Gravley, D.M., Wilson, C.J.N., Rosenberg, M.D., Leonard G.S.: The nature and age of Ohakuri Formation and Ohakuri Group rocks in surface exposures and geothermal drillhole sequences in the central Taupo Volcanic Zone, New Zealand. *New Zealand Journal of Geology and Geophysics*, **49**, (2006), 305–308.

Guerriero, V., Vitale, S., Ciarcia, S., Mazzoli, S.: Improved statistical multi-scale analysis of fractured reservoir analogues. *Tectonophysics*, **504**, (2011), 14–24.

Horie, T., Muto, T.: The Worlds' Largest Single Cylinder Geothermal Power Generation Unit. *GRC Transactions, Vol. 34*, (2010), 1039-1044.

Hooker, J.N., Laubach, S.E., Marrett, R: Fracture-aperture size—frequency, spatial distribution, and growth processes in strata-bounded and non-strata-bounded fractures, Cambrian Mesón Group, NW Argentina. *Journal of Structural Geology*, **54**, (2013), 54–71.

Huang, Q., Angelier, J.: Fracture spacing and its relation to bed thickness. Geological Magazine, **126**, (1989), 355–362.

Hurst, A.W., Bannister, S.C., Robinson, R., Scott, B.: Characteristics of three recent earthquake sequences in the Taupo Volcanic Zone, New Zealand. *Tectonophysics*, **452**, (2008), 17–28.

Kolyukhin, D., Torabi, A.: Statistical analysis of the relationships between faults attributes. *Journal of Geophysical Research*, **117**, (2012), 1–14.

Ladeira, F.L., and N.J. Price, Relationship between fracture spacing and bed thickness, Journal of Structural Geology, **3**, (1981), 179-183.

Ledesert, B., Dubois, J., Genter, A., Meunier, A.: Fractal analysis of fractures applied to Soultz-sous-Forets hot dry rock geothermal program. *Journal of Volcanology and Geothermal Research*, **57**, (1993), 1 – 17.

Legmann, H., Sullivan, P.: The 30 MW Rotokawa I geothermal project five years of operation. *International Geothermal Conference, Reykjavik*, (2003), 26–31.

Lofts, J.C., Bourke, L.T.: The recognition of artefacts from acoustic and resistivity borehole imaging devices. *in: Lovell, M., Wiliamson, G., Harvey, P.K. (Eds.), Borehole Imaging: Application and Case Histories. Special Publication No. 159. The Geological Society Publishing House, London*, pp. 59–76, (1999).

Massiot, C., McNamara, D.D., Lewis, B., Price, L., Bignall, G.: Statistical corrections of fracture sampling bias in boreholes from acoustic televiewer logs. *Proceedings*, New Zealand Geothermal. Workshop (2012).

Massiot, C., McNamara, D.D., Lewis, B.: Processing and analysis of high temperature geothermal acoustic borehole image logs, New Zealand. *Geothermics*, **53**, (2015), 190-201.

McNamara, D.D., Massiot, C., Lewis, B., Wallis, I. C. (accepted): Heterogeneity of structure and stress in the Rotokawa Geothermal Field, New Zealand. *Journal of Geophysical Research*.

Narr, W., Suppe, J.: Joint spacing in sedimentary rocks. *Journal of Structural Geology*, **13**, (1991), 1037e1048.

Nicol, A., Walsh, J.J., Watterson, J., Gillespie, P.A.: Fault size distributions - are they really power law? *Journal Structural Geology*, **18**, (1996), 191-197.

Newman, M.: Power laws, Pareto distributions and Zipf's law. *Contemporary Physics*, **46**, (2005), 323–351.

Pickering, G., Bull, J.M., and Sanderson, D.J.: Sampling power-law distributions. *Tectonophysics* **248**, (1995), 1–20.

Priest, S. Discontinuity analysis for rock engineering. Chapman and Hall, (1993).

Priest, S., Hudson, J. a.: Estimation of discontinuity spacing and trace length using scanline surveys. *International Journal of Rock Mechanics and Mining Sciences & Geomechanics Abstracts*, 18, (1981), 183–197.

Quinao, J., Sirad-azwar, L., Clearwater, J., Hoepfinger, V., Brun, M. Le, Zealand, N.: Aalyses and modelling of reservoir pressure changes to interpret the Rotokawa Geothermal Field response to Nga Awa Purua power station operation. *Proceedings*, Thirty-Eighth Workshop on Geothermal Reservoir Engineering, Stanford University, Stanford. (2013).

Quinao, J., Sirad-azwar, L.: Correlation of reservoir monitoring and continuous production data to interpret unexpected well behavior in Rotokawa. *Proceedings*, New Zealand Geothermal. Workshop (2012).

Radilla, G., Sausse, J., Sanjuan, B., Fourar, M.: Interpreting tracer tests in the enhanced geothermal system (EGS) of Soultz-sous-Forêts using the equivalent stratified medium approach. *Geothermics*, **44**, (2012), 43–51.

Rae, A.: Rotokawa Geology and Geophysics. *GNS Science Consultancy Report*., (2007), 2007/83.

Rives, T., Razack, M., Petit, J.P., Rawnsley, K.D.: Joint spacing: analogue and numerical simulations. *Journal of Structural Geology*, **14**, (1992), 925–937.

Sasaki, M.: Statistical Features of Vein Systems in the Hishikari Epithermal Gold Deposit, Japan. *Resource Geology*, **56**, (2006),27–36.

Schwarz, G.: Estimating the dimension of a model, *The annals of Statistic*, 6(2), (1978), 461–464.

Siratovich, P.A., Davidson, J., Villeneuve, M., Gravley, D., Kennedy, B., Cole, J., Wyering, and L., Price, L.: Physical and mechanical properties of the Rotokawa Andesite from production wells RK 27_L2 , RK 28 and RK 30, *Proceedings*, New Zealand Geothermal. Workshop (2012).

Spörli, K.B., Rowland, J.V.: "Column on column" structures as indicators of lava/ice interaction, Ruapehu andesite volcano, New Zealand *Journal of Volcanology and Geothermal Research*, **157**, (2006), 294–310.

Stasinopoulos, D.M., Rigby, R.A.: Generalized Additive Models for Location Scale and Shape (GAMLSS), *Journal of Statistical Software*, **23-7**, (2007).

R Development Core Team: R: A language and environment for statistical computing. *R Foundation for Statistical Computing, Vienna, Austria* (2008). ISBN 3-900051-07-0, URL http://www.R-project.org.

Sewell, S.M., Cumming, W.B., Bardsley, C., Winick, J., Quinao, J., Wallis, I.C., Sherburn, S., Bourguignon, S., Bannister, S.C.: Interpretation of microearthquakes at the Rotokawa Geothermal Field, 2008 to 2012. *Proceedings*, New Zealand Geothermal. Workshop (2013).

Terzagui, R.D.: Sources of error in joint surveys. *Geotechnique*, **15**, (1965), 287–304.

Wallis, I.C., Bardsley, C., Powell, T., Rowland, J.V., Brien, J.M.O.: A structural model for the Rotokawa Geothermal Field, New Zealand. *Proceedings*, New Zealand Geothermal. Workshop (2013).

Wu, H., Pollard, D.D.: An experimental study of the relationship between joint spacing and layer thickness. *Journal of Structural Geology*, **17**, (1995), 887–905.

Zuquim, M., Rowland, J.V.: Structural controls on fluid flow at the Onemana area, Coromandel Peninsula, New Zealand. *Proceedings*, New Zealand Geothermal. Workshop (2013).

APPENDIX

Appendix 1: Formulation of the probability density functions of the statistical distributions used in this study.

Distribution	Probability density function
Exponential	$f_y(y\|\lambda) = \lambda \exp(-\lambda y) \quad \text{for } y > 0,\ \lambda > 0$
Gamma	$f_y(y\|\mu,\sigma) = \frac{1}{(\sigma^2\mu)^{\frac{1}{\sigma^2}}} \frac{y^{\frac{1}{\sigma^2}-1} \exp -\frac{y}{\sigma^2\mu}}{\Gamma(\frac{1}{\sigma^2})} \quad \text{for } y > 0,\ \mu > 0 \text{ and } \sigma > 0$
Log-normal	$f_y(y\|\mu,\sigma) = \frac{1}{y\sqrt{(2\pi)\sigma}} \exp -\frac{1}{2}(\frac{\log y-\mu}{\sigma})^2 \quad \text{for } y > 0,\ \mu \in (-\infty,+\infty) \text{ and } \sigma > 0$
Power-law	$f_y(y\|\mu,\sigma) = \frac{1}{\sigma}\mu^{\frac{1}{\sigma}}(y+\mu)^{-\frac{1}{\sigma}+1}$ (Pareto II) $\quad \text{for } y \geq 0,\ \mu > 0 \text{ and } \sigma > 0$ $f_y(y\|\alpha) = \alpha y_{min}^{\alpha} y^{-(\alpha+1)} \quad \text{where } \alpha = \frac{1}{\sigma}$ (Power-law)
Power-exponential	$f_y(y\|\mu,\sigma,\nu) = \frac{\frac{1}{\sigma}(\nu \exp -0.5*\|z/c\|^{\nu})}{c*2^{1+\frac{1}{\nu}}*\Gamma(\frac{1}{\nu})} \quad \text{where c}= [\frac{2^{-\frac{2}{\nu}}\Gamma(\frac{1}{\nu})}{\Gamma(\frac{3}{\nu})}]^{0.5}$ $\text{for } y \in (-\infty,+\infty),\ \mu \in (-\infty,+\infty),\ \sigma > 0 \text{ and } \nu > 0$